Surface electron-energy-loss fine-structure investigation on the local structure of copper clusters on graphite

M. De Crescenzi,* M. Diociaiuti, L. Lozzi, P. Picozzi, and S. Santucci
Dipartimento di Fisica, Universitá dell'Aquila, 67100 L'Aquila, Italy
(Received 19 November 1986)

The lattice parameters of copper clusters deposited on graphite substrates were determined by surface extended energy-loss fine-structure measurements. The Fourier analysis of the fine structures beyond the $M_{2,3}$ copper edge shows a sizable lattice-parameter contraction when the cluster mean diameter $\bar{d}$ decreases. This contraction amounts to 4.7% for the particles with $\bar{d}=9$ Å. The contraction is linearly dependent on $1/\bar{d}$, which is why it was interpreted in terms of the liquid-drop model. Moreover, the observed strong enhancement of the Debye-Waller factor allowed us to estimate the decrease in melting point for small clusters. The sizable changes in the nearest-neighbor distance of our clusters are closely related to the change in the near-$L_{2,3}$-edge features. Our results are in good agreement with recent density-of-state calculations for compressed Cu crystals.

I. INTRODUCTION

During the last few years there has been an increasing interest in determining the lattice parameter variations occurring in metal clusters with the varying of the mean diameter $\bar{d}$.[1-4] Generally, a lattice contraction was observed according to the macroscopic liquid-drop model.[5] This model provides a dependence of this contraction on $1/\bar{d}$ which is proportional to the cluster ratio between surface and volume.

In the past, the cluster lattice-parameter measurement was made using electron[6,7] and x-ray[8] diffraction techniques. Recently, the use of extended x-ray-absorption fine-structure (EXAFS) spectroscopy provided an accurate tool for local structure of small clusters.[1-4] The results obtained by means of both techniques generally agree for a wide variety of metal clusters.

In the case of copper, however, there is a wide range of reported data varying from null[7] to a few percent lattice-parameter reduction.[1] Very recently, Montano *et al.*[9] reported on an EXAFS experiment on copper clusters isolated in solid argon. Their results clearly show an appreciable lattice-parameter reduction only for very small copper molecules Cu_2.

In order to determine the actual amount of contractions, we performed a structural investigation by means of the surface electron-energy-loss fine-structure (SEELFS) technique which has a good surface sensitivity and provided structural results similar to those obtained by EXAFS.[10,11]

The SEELFS technique allows us to determine the local structure of clusters deposited on weakly interacting substrates because the aggregates are not embedded in matrix (amorphous carbon or solid rare gases) as required by the previously reported structural techniques.

In this paper we report on a complete investigation of the lattice-parameter contraction of copper clusters whose real mean diameters were determined by Auger spectra and electron microscopy analysis.

The Fourier transform of the SEELFS data, above the $M_{2,3}$ Cu edge, shows a linear contraction in the nearest-neighbor distances up to 4.7% for the clusters with a mean diameter of 9 Å.

One of the significant results of this work is a sizable enhancement of the mean-square fluctuation in the interatomic distance which is related to the Debye-Waller factor. Inserting the values in the Lindemann's fusion formula recently developed by Solliard for clusters[12] we found a lowering (a factor of 2) in the melting point of smallest clusters.

Furthermore, a careful analysis of $L_{2,3}$-near-edge features of our SEELFS spectra shows a sizable shift (up to 10 eV) towards higher binding energies. This shift is closely related to the changes in the density of states above E_F due to the contraction of nearest-neighbor distance in the Cu clusters. This observation is in good agreement with the recent calculation by Albers *et al.*[13] for compressed Cu bulk.

This paper is outlined as follows. In Sec. II we describe the apparatus needed to detect the SEELFS features and present experimental results. In Sec. III we briefly discuss the theoretical scheme which leads to an EXAFS-like formulation of the scattering cross section measured in a SEELFS experiment. Finally, in Sec. IV we discuss the prominent structure and compare our results to some previous measurements.

II. EXPERIMENTAL DETAILS

A. Apparatus

Clusters were prepared by evaporating copper (99.99% pure) from a tungsten wire onto a clean polycrystalline graphite substrate and grids with carbon at room temperature in a UHV chamber with a base pressure in the 10^{-10}-torr range. The nominal thicknesses were monitored by an Inficon quartz microbalance. Transmission electron microscopy was used to determine the cluster di-

mensions and the fraction of the surface covered with clusters.

The vacuum chamber was equipped with a Riber single-pass cylindrical mirror analyzer (CMA) for electron spectroscopy measurements. The energy resolution $\Delta E/E$ was about 0.3%. A primary-electron energy of about 2000 eV was used with a beam current of 1 μA. Peak-to-peak modulation voltage from 1 to 7 V was applied to CMA to obtain Auger and SEELFS signals. Signals were detected with a lock-in amplifier recording the first derivative of the electron yield distribution $[dN(E)/dE]$.

Data acquisition was performed with the help of an IBM PC interfaced to the lock-in amplifier. The full energy range of a given scan was swept at least three times in order to achieve a satisfactory signal-to-noise ratio. The collection time for each run was about 15 min.

B. Cluster mean diameter determination

Many difficulties in determining the lattice parameter contraction law are due to accuracy in the cluster mean diameter $\bar{d}$ measurements. In our work we used Auger spectra as a quantitative analysis of the mean size following a procedure described by Memeo *et al.*[14] This method is based only on the ratio R between the Auger peak intensities of copper I_{Cu} and carbon I_C. R is given by[14]

$$R=\frac{I_{Cu}}{I_C}=\frac{x[1-\exp(-hd_{Cu}/\lambda_{Cu})]}{[1-\exp(-d_{Cu}/\lambda_{Cu})][1-x+x\exp(-hd_C/\lambda_C)]G}, \quad (1)$$

where x is the fraction of area covered with clusters, h is an integer equal to the number of deposited layers, d is the distance between two consecutive atomic layers, λ is the mean free path in the material of the Auger electrons, and G is given by

$$G=\frac{1}{1-\exp(-d_C/\lambda_C)}.$$

Cu and C refer to copper and carbon. Except for x, whose values were measured from electron micrographs, all other quantities were directly obtained from the Auger spectra.

The application of this procedure is justified because the Auger line shapes for both metal deposits and carbon substrates do not change as the coverage increases, due to the absence of compound formation.

The Auger spectra of clean graphite and Cu deposits with nominal thicknesses 1, 3, 6, 12, 20, and 60 Å were collected into the range 0—1000 eV. The clean substrates showed only the presence of a carbon KVV transition while the subsequent Cu growth appeared as an increasing structure at about 60 eV (MVV transitions) and between 700—900 eV (LVV transitions). The presence of the graphite K edge in all the spectra except for the bulk reassured about the Cu island growth.[15]

Figure 1(a) shows the peak-to-peak intensities of copper and graphite as a function of the nominal coverage of deposits. Figure 1(b) shows the R ratio obtained from our Auger data (circles). From the fitting of our R results by means of Eq. (1), using the experimental values of x, we obtain the equivalent mean diameters of clusters reported in the lower scale of Fig. 1(b). The dotted line shows the theoretical R ratio expected from a layer-by-layer Cu growth on graphite versus the nominal coverage. There is a good agreement between the mean diameters obtained by this calibration procedure and those measured from the distribution of the cluster diameters obtained by TEM.

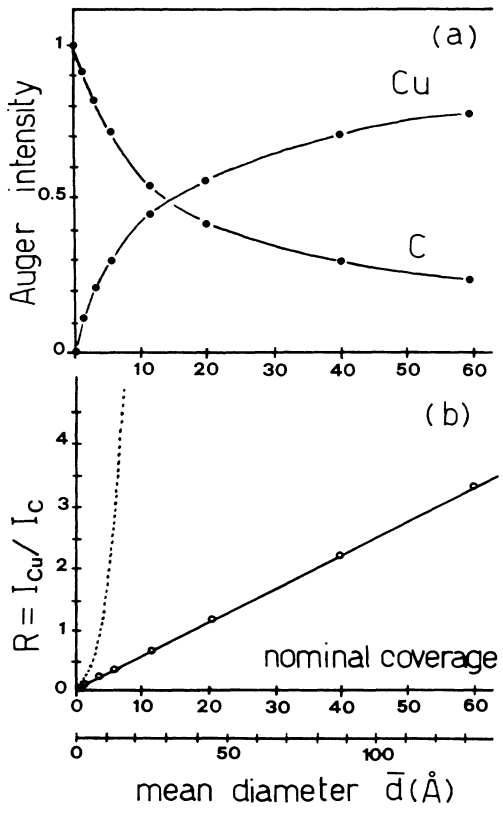

FIG. 1. (a) Peak-to-peak normalized Auger intensity for graphite (CVV transitions) and copper clusters (LVV transitions) vs the nominal thickness. (b) Peak-to-peak intensity ratio ($R=I_{Cu}/I_C$) from (a) (circles). The solid line is the fit curve obtained from Eq. (1) supposing a cluster growth vs the cluster mean diameter. For the area fraction x covered by discontinuous film with nominal thicknesses 1, 3, 6, 12, 20, 40, and 60 Å we used the following values: 0.05, 0.1, 0.2, 0.24, 0.34, 0.41, and 0.5, respectively. The dotted line shows the theoretical ratio relative to layer-by-layer growth using Eq. (1) (Ref. 14).

III. CORRESPONDENCE BETWEEN EXAFS AND SEELFS SPECTROSCOPIES

Electron-energy-loss spectroscopy was used to excite the inner core electrons and the related extended fine structures mainly in the transmission mode (EXELFS).[16] This technique showed a close correspondence with the EXAFS technique.[16]

Recently, the electron-energy-loss technique was used in the reflection mode.[10,11] The important difference between the transmission and reflection modes is the possibility for the latter of using a conventional Auger apparatus available in any surface science laboratory. While on one hand the use of low primary beam energies allows us to enhance the surface sensitivity, on the other, it should dissipate all doubts about the validity of the so-called dipole approximation which is well accepted in the EXELFS spectroscopy.

In fact, the cross section for an electron with energy E_p which excites a core electron gaining an energy ΔE and momentum q is given by[16]

$$\frac{d^2\sigma}{\Delta E\, dq}=\frac{8\pi e^4}{\hbar^2 v^2 q^3}\,|\langle\psi_f|e^{i\bar{q}\cdot\bar{r}_c}|\psi_i\rangle|^2\,, \tag{2}$$

where the Born approximation is supposed to be valid, v is the velocity of the incident electron, and r_c is the core radius. The measured cross section is proportional to the integral of equation (2) between $q_{\min}$ and $q_{\max}$, depending on the angular collection geometry. Simple considerations on the reflection scattering lead to a definition of a $q_{\min}\simeq\sqrt{0.263}[(E_p)^{1/2}-(E_p-\Delta E)^{1/2}]$ and $q_{\max}\simeq\sqrt{\Delta E}$.[17] Moreover, one should note that the $1/q^3$ dependence on the cross section strongly enhances the values around $q_{\min}$. This is particularly verified in our case because the CMA analyzer integrates on all possible $\bar{q}$ values.

In our case $E_p=2000$ eV, $\Delta E=200$ eV ($M_{2,3}$ extended features), $q_{\min}=1.18$ Å^{-1}, and $r_c=0.23$ Å. As a consequence, $qr_c<1$ and developing the electron operator, neglecting the higher-order terms, we obtain[10]

$$\frac{d\sigma_{\rm if}}{d(\Delta E)}\simeq|\langle\psi_f|\bar{\epsilon}_q\cdot\bar{r}_c|\psi_i\rangle|^2\int_{q_{\min}}^{q_{\max}}\frac{dq}{q}\,, \tag{3}$$

which is very close to the x-ray matrix element. Here, $\bar{\epsilon}_q$ is the unit vector of the momentum transfer $\bar{q}$ and plays the same role as the electron field polarization.

On the basis of the above considerations we expect a good correspondence between reflection core-edge losses and photoabsorption spectra. For energy losses higher than the absorption edge, the final continuum state ψ_f must be constructed as an electronic wave that comes from the excited atomic level and backscattered part of this wave due to the presence of the neighbor atoms in the solid. This final-state definition, which produces the EXAFS features above the x-ray edges,[16] will also appear in the reflection electron-energy-loss spectra.

IV. STRUCTURAL PARAMETERS

A. Nearest-neighbor distance determination

Figure 2 shows the SEELFS spectra above the $M_{2,3}$ edge of copper films with nominal thicknesses 3, 6, 12, 20, and 60 Å (cluster mean diameters of 9, 12.5, 25, 44, and 120 Å, respectively, correspond to these nominal thicknesses) and bulk. The energy-loss spectra were detected using the same experimental settings as those in the energy range up to 250 eV above the edge.

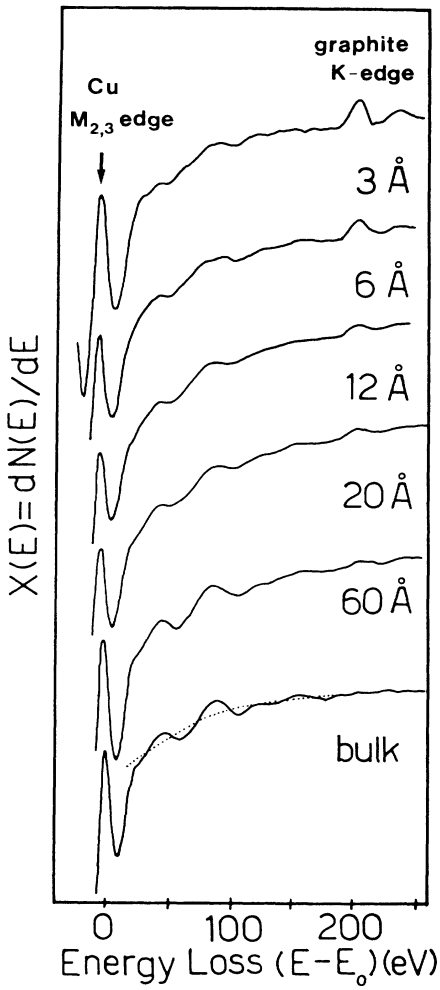

FIG. 2. Electron-energy-loss features above the $M_{2,3}$ core edge for copper films with different nominal thicknesses and copper bulk. The dotted line for bulk represents the atomic background.

Figure 3 shows the SEELFS modulating signals obtained from data of Fig. 2 after subtracting a smooth background. This background is indicated for the bulk by the dotted line of Fig. 2. Only the energy range up to 200 eV above the edge is displayed in order to avoid the superposition with the graphite K edge located at 285 eV binding energy.

The spectra of Fig. 3 were transformed into $\chi(k)$ spectra, where $k=[0.263(E-E_0)]^{1/2}$ is the wave vector of the excited core electron above the edge E_0 and $E-E_0$ is the energy loss. The data were then analyzed using the EXAFS theory which describes the signals by means of the following equation:[16]

$$\chi(k)=\sum_j \tilde{A}_j(k)\sin[2kR_j+\Phi_j(k)]\,. \tag{4}$$

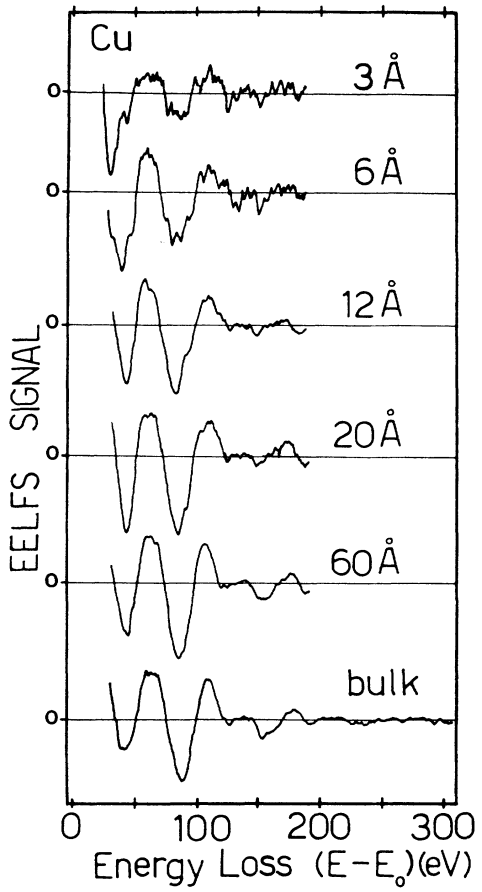

FIG. 3. SEELFS signals extracted from Fig. 2 for the same samples. All spectra are limited up to about 200 eV above the Cu $M_{2,3}$ edge in order to avoid the superposition with the substrate graphite K edge.

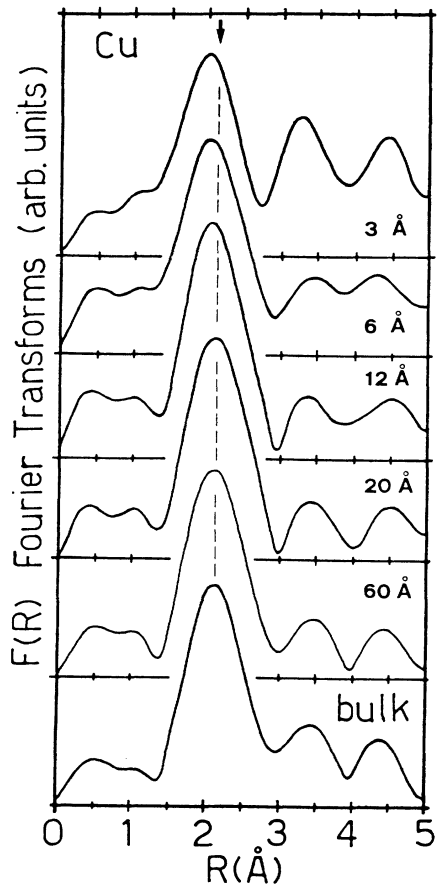

FIG. 4. Fourier integration of SEELFS spectra shown in Fig. 3. In the figure the nominal thickness is indicated. The dashed line and the arrow indicate the bulk position of the first-nearest neighbors. Data are not corrected for the EXAFS phase shift.

The Fourier integration of the $\chi(k)$ directly gives the radial structure function $F(R)$, where R_j is the distance of the surrounding shell j from the excited atom minus a phase shift $\Phi_j(k)$. Figure 4 shows the Fourier integrations of the SEELFS results shown in Fig. 3 as a function of the real space. For the bulk, the main peak is located at 2.12 ± 0.02 Å. It should correspond to the twelve nearest-neighbor distances in the fcc Cu structure which are located at 2.55 Å.[18] The difference which amounts to 0.43 Å, is due to the EXAFS phase-shift correction.[19] This phase shift may be experimentally determined by the back-Fourier inversion of the main peak of $F(R)$, using the following equation:

$$\Phi_1(k)=\arctan\left[\frac{\mathrm{Re}[\chi(k)]}{\mathrm{Im}[\chi(k)]}\right]-2kR_1\ , \tag{5}$$

where $\chi(k)$ is the contribution of the SEELFS signal due to the first shell only and R_1 is the crystallographic distance. For the bulk we obtain a straight line fitted by the following equation:

$$\Phi_1(k)=-0.86k+5.1\ . \tag{6}$$

We note from Fig. 4 that the main peak position of the Fourier transforms shifts dramatically towards lower distances when the film thickness decreases. For the thinnest films we observe a value of 2.00 Å denoting a 4.7%

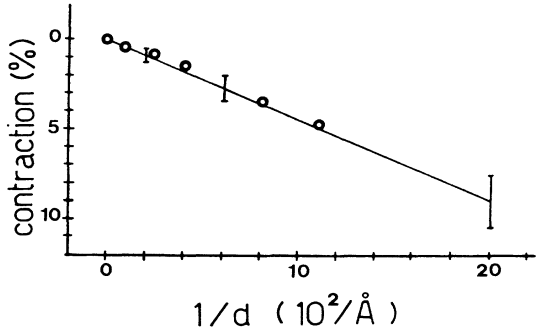

FIG. 5. Plot of percentage decrease in near-neighbors distance vs the reciprocal of the diameter d for different Cu clusters (circles) obtained from the $F(R)$ analysis of Fig. 4. The solid line represents the EXAFS results of Apai *et al.* (Ref. 1).

nearest-neighbor contraction.

Assuming the complete phase-shift transferability[20] for the Cu-pair atoms we must change R_1 in Eq. (5) in order to obtain the same slope of Eq. (6), for the clusters too. Figure 5 shows the observed contraction versus the inverse of the cluster mean diameter (circles) together with the result obtained by EXAFS measurements reported by Apai[1] (solid line).

B. Debye-Waller factor results

Besides the structural information in terms of $F(R)$ for different clusters, the analysis of the extended energy-loss features allows us to determine some other significant parameters such as the Debye-Waller factors.

It is well known that the atoms located at or near the surface of the cluster have vibrational properties greatly differing from those of the bulk atoms. Theory predicts that the mean-square fluctuations in the interatomic distances for the surface atoms increase considerably.[12,21] For all clusters observed, the ratio between the number of surface and bulk atoms ranges from 0.76 ($\bar{d}=9$ Å) to 0.31 ($\bar{d}=40$ Å); therefore, many atoms should have a higher Debye-Waller factor as compared to that of the bulk.

In order to check these cluster properties and the sensitivity of our technique to the variations of the atomic vibrations in the cluster, we analyzed our results following the procedure described by Greegor and Lytle.[22] Namely, the main peak of $F(R)$ of Fig. 4 was back-Fourier-filtered in order to obtain the amplitude function $\tilde{A}(k)$. The results for different clusters are reported in Fig. 6(a).

The EXAFS theory describes $\tilde{A}(k)$ with the following equation:[19]

$$\tilde{A}_1(k)=\frac{1}{k}\frac{N_1}{R_1^2}F(k,\pi)e^{-2\sigma^2k^2}e^{-2R_1/\lambda}, \tag{7}$$

where N_1 is the number of atoms in the shell 1, R_1 is the distance to the shell 1 from the central atom, σ^2 is the mean-square deviation of the interatomic distance R_1, and $F(k,\pi)$ is the backscattering function. The comparison of the backscattering functions for bulk and cluster, assuming a complete backscattering function transferability,[20] allows differences in the Debye-Waller factors to be determined using the equation[22]

$$\ln\frac{\tilde{A}_b(k)}{\tilde{A}_c(k)}=2(\sigma_c^2-\sigma_b^2)k^2+\ln\frac{N_b}{N_c}\left[\frac{R_c}{R_b}\right]^2, \tag{8}$$

where the subscripts b and c refer to the bulk and cluster, respectively.

In Fig. 6(a) we show the different backscattering amplitudes $\tilde{A}(k)$, while in Fig. 6(b) we report the variation of the Debye-Waller factors according to Eq. (8). Extrapolation of curves of Fig. 6(b) to zero value should give information on the variation of the coordination number N. In Fig. 7 we report the difference $\Delta\sigma^2=\sigma_c^2-\sigma_b^2$, which indicates the increasing dynamic disorder of surface atoms, as a function of the cluster mean diameter. Assuming for σ_b^2 the value 7.7×10^{-3} Å^2, the Debye-Waller factor for the smallest cluster is about twice that of the bulk.

Recently, Solliard[12] on the basis of Lindemann's criterion for melting point found the following relationship containing the Debye-Waller factors and some character-

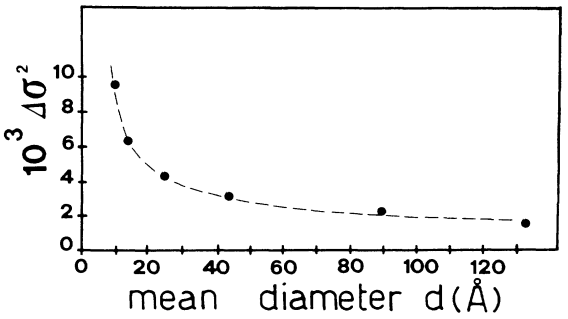

FIG. 7. $\Delta\sigma^2=\sigma_c^2-\sigma_b^2$ for different Cu clusters, vs mean diameter, obtained from slopes of curves of Fig. 6(b).

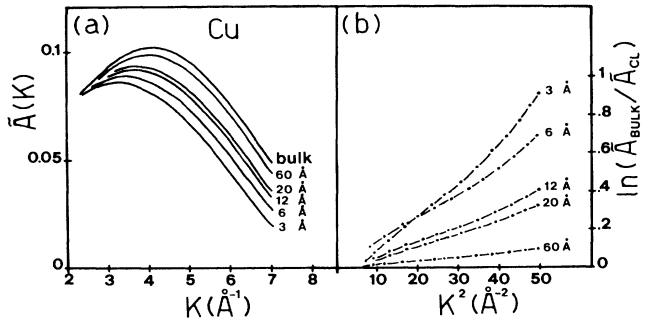

FIG. 6. (a) Envelope functions of different Cu clusters as obtained from the back-Fourier-filtering of the first-nearest-neighbor peak of $F(R)$ of Fig. 4. (b) Logarithm of the ratio of envelope functions of (a).

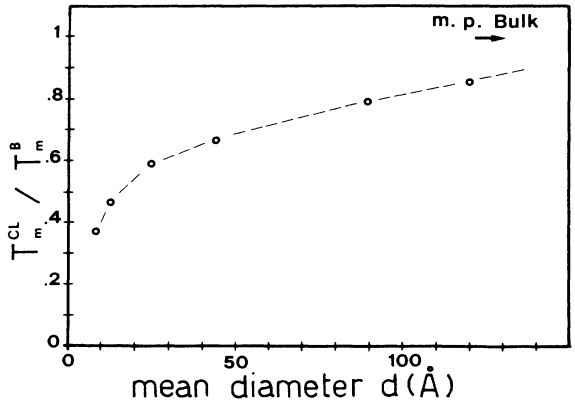

FIG. 8. Melting temperature of small Cu particles obtained using Eq. (12) (Ref. 12) based on the Lindemann's melting criterion. The experimental lattice parameter and mean relative displacements were used.

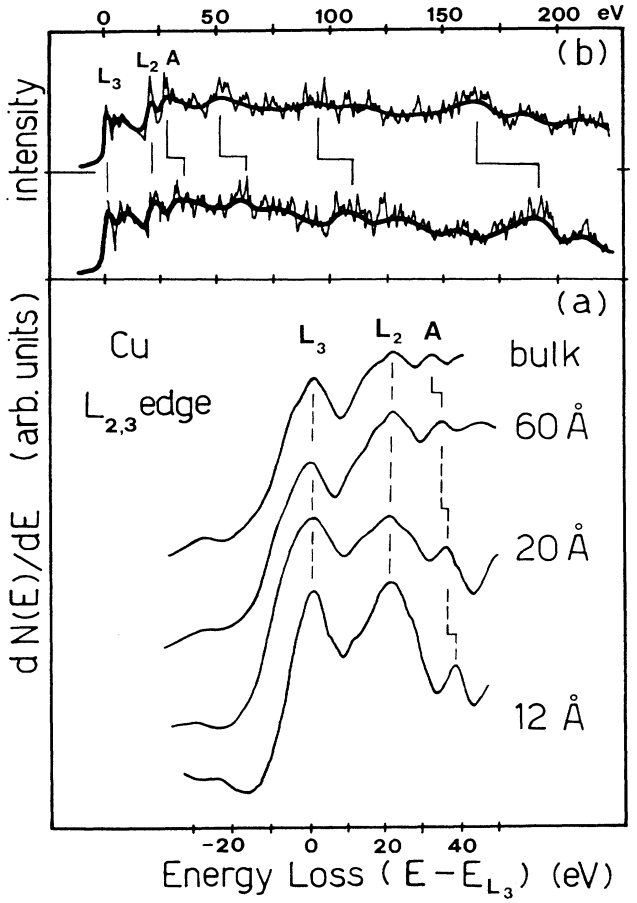

FIG. 9. (a) Experimental near-edge energy-loss feature above Cu $L_{2,3}$ edges for different Cu deposits. Note that the feature A shifts towards high binding energies, decreasing the cluster size. (b) $L_{2,3}$ absorption coefficient obtained by Albers and coworkers (Ref. 13) through band-structure calculations including the partial density of states. The upper curve has been calculated for the uncompressed bulk while the lower curve for the compressed one ($V/V_c=1.3$).

izing cluster parameters:

$$\frac{T_m^c}{T_m^b}=\left[1-\frac{4\kappa\gamma}{3d}\right]\frac{\beta^b(T_m^b)}{\beta^c(T_m^c)}\ , \tag{9}$$

where T_m^c and T_m^b are the cluster and bulk melting temperatures, respectively, γ is the surface stress, κ is the compressibility, and d is the cluster mean diameter and

$$\beta=\frac{4\pi^2\langle u^2\rangle}{a^2T}\ ,$$

where a is the lattice parameter, $\langle u^2\rangle$ is the mean-square atomic vibration amplitude, and T is the temperature. Our measurements of lattice-parameter contraction, shown in Fig. 5, confirm that the liquid-drop model is also satisfactory for copper clusters. In this model

$$\frac{\Delta a}{a}=-\frac{4\kappa\gamma}{3d}\ . \tag{10}$$

The experimental relative variation of the lattice parameter as reported in Fig. 5 allows us to determine the first term of the second member of Eq. (9). Substituting the above results in Eq. (9) and assuming that[21]

$$\langle u^2\rangle\simeq 2\langle\sigma^2\rangle \tag{11}$$

for the melting temperature of the cluster, we obtain the following equation:

$$T_m^c=T_m^b\left[\frac{a_c}{a_b}\right]^3\left[\frac{\sigma_b}{\sigma_c}\right]^2\ . \tag{12}$$

In Fig. 8 we reported the melting temperature results for our examined clusters. A very similar behavior was observed by Buffat[23] for gold clusters.

C. Near-edge structures

One should expect that the lattice-parameter variations produce sizable changes also in the electronic properties of clusters. On the other hand, strong variations of the d band in Cu clusters were observed by photoemission on different substrates[24,25] and with Auger measurements.[26]

A similar behavior should also be observed for the empty states above E_F. Energy-loss measurements in the near-edge region provide a tool for investigating any variations occurring in these states of clusters, similar to the x-ray-absorption near-edge-structure spectroscopy.[27] In fact, in this region, due to the higher mean free path, the single-scattering approach which leads to the EXAFS formula does not hold and the structure above the edge may be interpreted on the basis of a full band-structure theory[13] as well as in the multiple-scattering approach.[28]

In Fig. 9(a) we report our energy-loss spectra in the region around the $L_{2,3}$ edges which involve mainly $p\rightarrow d$ transitions. We observe that, when the cluster mean diameter decreases, the edges do not shift while structure A moves towards higher binding energies. This shift amounts to 6 eV for the smallest clusters.

Recently, Albers *et al.*[13] performed a band-structure calculation for copper in different conditions of hydrostatic pressure. In Fig. 9(b) their partial density of states $p\rightarrow d$ is shown which reproduces the x-ray absorption for uncompressed (upper curve) and compressed (lower curve) copper bulk. The reported amount of compression $V/V_c=\frac{1}{3}$ corresponds to a reduction in lattice parameter of 8%. The reported data of Albers *et al.* show an increased shift of the structures between 25 and 200 eV. Focusing our attention on the structure around 30 eV above E_{L_3}, we observe that it shifts by the same order of magnitude as the smallest clusters. This confirms that the lattice-parameter contraction produces a sizable variation also in the empty states above E_F.

V. CONCLUSIONS

We have shown that the SEELFS measurements are a sensitive tool for determining the structural and electronic variations occurring in the clusters. While the greatest lattice-parameter contraction of 4.7% is in good agreement with the EXAFS results reported by Apai *et al.*, it strongly differs from recent x-ray diffraction[8] and

EXAFS[9] measurements. On the other hand, the good agreement between the measured and calculated shift of the structures above the $L_{2,3}$ edge is good evidence that the narrowing of the lattice parameter is a genuine effect occurring when the cluster size is reduced. Finally, we suggest the SEELFS technique as a very simple method to estimate the melting-point temperature of the small clusters based on the measurements of the Debye-Waller factor variations.

ACKNOWLEDGMENTS

The authors are grateful to L. Paoletti for electron microscopy analysis performed at the Istituto Superiore di Sanitá, and to O. Consorte for technical assistance. This work was supported by the Consiglio Nazionale delle Ricerche through the Gruppo Nazionale di Struttura della Materia.

---

*Present address: Department of Physics, Roma II University, Tor Vergata, 00173 Roma, Italy.

[1]G. Apai, J. F. Hamilton, J. Stöhr, and A. Thompson, Phys. Rev. Lett. **43**, 165 (1979).
[2]B. Moraweck and A. J. Renouprez, Surf. Sci. **35**, 106 (1981).
[3]A. Balerna, E. Bernieri, P. Picozzi, A. Reale, S. Santucci, E. Burattini, and S. Mobilio, Phys. Rev. B **31**, 5058 (1985).
[4]P. A. Montano, W. Schulze, B. Tesche, G. K. Shenoy, and T. I. Morrison, Phys. Rev. B **30**, 672 (1984).
[5]C. W. Mays, J. S. Vermaak, and D. Kuhlmann-Wilsdorf, Surf. Sci. **12**, 128 (1968); **12**, 134 (1968).
[6]H. J. Wasserman and J. S. Vermaak, Surf. Sci. **22**, 164 (1970).
[7]H. J. Wassermann and J. S. Vermaak, Surf. Sci. **32**, 167 (1972).
[8]W. Vogel, Surf. Sci. **156**, 420 (1985).
[9]P. A. Montano, J. K. Shenoy, E. E. Alp, W. Schulze, and J. Urban, Phys. Rev. Lett. **56**, 2076 (1986).
[10]M. De Crescenzi and G. Chiarello, J. Phys. C **18**, 3594 (1985), and references therein.
[11]M. De Crescenzi, G. Chiarello, E. Colavita, and R. Memeo, Phys. Rev. B **29**, 3730 (1984).
[12]C. Solliard, Solid State Commun. **51**, 947 (1984), and references therein.
[13]R. C. Albers, A. K. McMahan, and J. E. Müller, Phys. Rev. B **31**, 3435 (1985).
[14]R. Memeo, F. Ciccacci, C. Mariani, and S. Ossicini, Thin Solid Films **109**, 159 (1983).
[15]M. De Crescenzi, P. Picozzi, S. Santucci, C. Battistoni, and G. Mattogno, Solid State Commun. **51**, 811 (1984).
[16]See, for example, *EXAFS Spectroscopy and Related Techniques*, edited by B. K. Teo and D. C. Joy (Plenum, New York, 1980); R. D. Leepman, L. A. Grunes, and P. L. Feyes, Phys. Rev. B **26**, 614 (1982).
[17]A. G. Nassiopoulos and Cazaux, Surf. Sci. **149**, 313 (1985).
[18]R. W. G. Wyckhoff, *Crystal Structures* (Interscience, New York, 1980).
[19]P. A. Lee, P. H. Citrin. P. Eisenberger, and B. M. Kincaid, Rev. Mod. Phys. **53**, 769 (1981).
[20]P. H. Citrin, P. Eisenberger, and B. M. Kincaid, Phys. Rev. Lett. **36**, 1346 (1976).
[21]D. P. Jackson, Surf. Sci. **43**, 431 (1974); G. Treglia and M. C. Desjonqueres, *ibid.* **162**, 126 (1985).
[22]R. B. Greegor and G. W. Lytle, Phys. Rev. B **20**, 4902 (1979).
[23]Ph. Buffat and J. P. Borel, Phys. Rev. A **13**, 2287 (1976).
[24]W. F. Egelhoff, Jr. and G. G. Tibbets, Phys. Rev. B **19**, 5028 (1979).
[25]W. F. Egelhoff, Jr., J. Vac. Sci. Technol. **20**, 668 (1982).
[26]M. De Crescenzi, M. Diociaiuti, L. Lozzi, P. Picozzi, and S. Santucci, Surf. Sci. **178**, 282 (1986).
[27]See *EXAFS and Near Edge Structure*, edited by A. Bianconi, L. Incoccia, and S. Stipcich (Springer, Berlin, 1983).
[28]J. N. Greaves, P. J. Durham, J. Diacun, and P. Quinn, Nature **294**, 139 (1981).